A SURVEY ON RECENT DEVELOPMENTS IN SECOND-ORDER INTEGRATION METHODS FOR J_2 PLASTICITY MODEL

Edoardo Artioli[1,2] - Ferdinando Auricchio[1,2] - Lourenço Beirão da Veiga [3]

[1] IMATI-CNR, Via Ferrata 1, 27100 Pavia, Italy

[2] Department of Structural Mechanics, University of Pavia, Via Ferrata 1, 27100 Pavia, Italy

[3] Departmen of Mathematics, University of Milan, Via Saldini 50, 20133 Milano, Italy

artioli@imati.cnr.it (Edoardo Artioli)

Abstract

In this paper we propose a survey on recently studied integration methods for elasoplasitc constitutive models. In particular, the von-Mises elastoplastic constitutive model in the realm of small deformations is considered. The model takes into account both linear isotropic hardening and linear/nonlinear kinematic hardening. The aim of the work is to present and compare a set of quadratically accurate integration algorithms based on different numerical strategies. Namely, we present two sets of algorithms: The first set is related to algorithms based on classical backward-Euler and midpoint integration schemes in conjunction to a standard return map procedure. The second set refers to newly developed integration schemes based on an ad hoc rewriting of the constitutive model by means of an integration factor governing the evolution process, coupled with the use of exponential maps for the time integration. The two class of methods analyzed above apply both to linear kinematic hardening model and nonlinear kinematic hardening models. The comparison of the different methods is then carried out by testing accuracy and precision using different time discretizations on mixed stress-strain loading histories adopting an overkilling reference solution computed via return map method. A technical problem solved through a finite element approach is presented in order to compare algorithms performance on a typical boundary value problem.

Keywords: Plasticity, Integration algorithm, Midpoint rule, Exponential map.

Presenting Author's biography

Edoardo Artioli took his master in Civil Engineering and PhD in Structural Mechanics from the University of Bologna, Italy. Now he is a post doc at the Institute for Applied Mathematics and Information Technology of Pavia, Italy and a member of the research group in Advanced Materials and Computational Mechanics at the EUCENTRE, Pavia.

1 Introduction

The present paper focuses on a class of newly developed integration algorithms for the J_2 or von-Mises elastoplastic constitutive model. The considered three dimensional constitutive model is set in the framework of infinitesimal strain regime and specializes to two main cases: associative case and non-associative case depending of the kind of hardening mechanism considered, i.e. on the type of rate equation assumed for the backstress internal variable. In the first case the backstress tensor evolves in time remaining normal to the yield surface in stress space, on the contrary this does not hold true for the nonassociative case in which the backstress evolution is depending on the backstress itself. In the first instance we speak of a combined linear isotropic and kinematic hardening model, in the second one of a combined linear isotropic-nonlinear kinematic hardening model. The form assumed for the hardening mechanism in the nonlinear case is due to Armstrong and Frederick [1] and is a very classical and established one.

The presented algorithms are subdivided in two main groups according to the solution strategy for the evolution equations, i.e. according to the time integration rule adopted. We thus split the presented methods in two main classes, namely midpoint-based methods and exponential-based methods. The first group contains a number of procedures which are based on finite difference-type integration rules and precisely on different versions of classical midpoint integration rule. These kind of methods apply the a standard return map concept for the solution of the final algebraic problem [2-4]. The midpoint schemes presented in the following section are suitable both to the associative case and to the nonassociative one.

The second group, instead, contains a set of newly developed algorithms which are baed on re-writing the constitutive model equations in terms of a scalar integration factor which is chosen to govern the evolution of the yield surface radius and by the construction of an augmented relative stress tensor. The constitutive model thus rewritten in the above terms shows a convenient quasi-linear form which is suitable for subsequent integration via exponential maps [5-7]. The exponential based methods herein presentd apply both to the associative case and to the nonassociative one.

The two sets of algorithms, even if completely different in principle, share a common feature, namely they are all second-order accurate schemes. With this we mean that the considered algorithms produce an error on the exact solution which decreases quadratically with respect to the time integration step size. This feature is of remarkable importance and represents a key point of these newly introduced schemes since most application and commercial codes implement just first-order accurate integration algorithms due to their relative coding simplicity and numerical robustness.

After a brief sketch of the considered classes of algorithms, we present numerical results both for the associative and the non-associative plasticity model. The numerical tests are carried out on pointwise stress-strain mixed loading history and on a boundary value equilibrium problem of an elastoplastic medium. The results are presented in order to give a comparison of the integration algorithms in terms of order of accuracy and precision and then to indicate the most efficient choice for practical simulation purposes.

2 Time-continuous model

Admitting a deviatoric/volumetric splitting of the stress tensor and of the strain tensor, the equations for the model under consideration are

$$p = K\theta \tag{1}$$

$$\mathbf{s} = 2G\left[\mathbf{e} - \mathbf{e}^p\right] \tag{2}$$

$$\boldsymbol{\Sigma} = \mathbf{s} - \boldsymbol{\alpha} \tag{3}$$

$$F = \|\boldsymbol{\Sigma}\| - \sigma_y \tag{4}$$

$$\dot{\mathbf{e}}^p = \dot{\gamma}\mathbf{n} \tag{5}$$

$$\sigma_y = \sigma_{y,0} + H_{iso}\gamma \tag{6}$$

$$\dot{\boldsymbol{\alpha}} = \dot{\gamma}H_{kin}\mathbf{n} - \dot{\gamma}H_{nl}\boldsymbol{\alpha} \tag{7}$$

$$\dot{\gamma} \geq 0, \quad F \leq 0, \quad \dot{\gamma}F = 0 \tag{8}$$

where K is the material bulk modulus, G is the shear modulus, $\mathbf{e}^p$ is the traceless plastic strain, $\boldsymbol{\alpha}$ is the backstress, $\boldsymbol{\Sigma}$ is the relative stress, F is the von Mises yield function, $\mathbf{n}$ is the normal to the yield surface, σ_y is the yield surface radius, the initial yield stress, H_{kin}, H_{iso} and H_{nl} are respectively the linear kinematic and isotropic hardening moduli and the nonlinear kinematic hardening modulus. Finally, Equations (8) represents the well known Kuhn-Tucker conditions which govern the loading-unloading conditions, making of the above set of equations a constrained evolution differential-algebraic problem. In what follows it is assumed that when the system is in an elastic phase $\gamma = 0$, while $\gamma > 0$, when the system is in a plastic phase.

We remark here that in the sequel we will treat both the case in which nonlinear kinematic hardening is present, for which case we say that we have a non-associative constitutive model and also the case in which H_{nl} is zero, in which case we have an associative model. From the theoretical and modeling standpoint there is a marked difference between the two cases and this becomes quite delicate in terms of designing integration algorithms architecture and evaluating the relative performance. Without going into too much details and referring the Reader to

specific literature for the detailed mathematical derivations, in the following, we will present integration algorithms specifically designed for the first kind of model and for the second one as well.

3 Second-order integration algorithms

3.1 Integration strategy and solution

In the sequel we assume to consider the problem of integrating the model represented by equations (3)-(9) under the consistency conditions (10), for a prescribed mixed stress-strain loading history taking place during the closed and bounded time interval $[0, T]$. Let us divide the time history interval $[0, T]$ into N sub-intervals defined by the points $0 = t_0 < t_1 < \ldots < t_n < t_{n+1} < \ldots < t_N = T$.

Given the history variable values $(\mathbf{s}_n, \boldsymbol{\alpha}_n, \mathbf{e}^p_n, \gamma_n)$ at time t_n, and the deviatoric strain $\mathbf{e}_{n+1}$ at time t_{n+1}, the problem consists in computing the history variables at time t_{n+1} consistently with the constitutive model. The strain history is assumed to be piecewise linear in time, while for simplicity the initial values for $\boldsymbol{\alpha}$, $\mathbf{e}^p$ and γ at t_0 are taken zero.

In the following sections we give a brief illustration of the two classes of second-order accurate integration algorithms for the considered model. Detailed mathematical derivations are omitted here for brevity's reasons but can be found in [5,6].

3.2 Midpoint rule integration algorithms

The midpoint-based algorithms considered for the J_2 associative model can be divided in two subsets:

• SMPT1 and SMPT2 single step algorithms [2,3,8]

• DMPT1 and DMPT2 double step algorithms [4,8]

The main difference between the two subets lies in the fact that the first two algorithms (single step algorithms) perform the updating of the history variables along a generic time interval with a single return map yield consistency condition enforcement, while the double step algorithms apply the return map twice over each update. The SMPT1 method applies a midpoint integration rule along the whole time interval and performs the return map at the end of the step. The SMPT2 method still applies a midpoint integration procedure over the entire time step, imposing the return map at the midpoint of the time integration interval. It is to be noted that whilst the SMPT1 guarantees yield consistency at the end of the time step, the SMPT2 method enforces yield consistency at the midpoint instant and is not therefore endpoint yield consistent. The SMPT2 scheme gives instead a simple nonlinear scalar problem for the plastic consistency parameter and a symmetric tangent operator which does not hold true for the SMPT1.

The algorithms grouped in the second subset are based on the idea of dividing each time step in two substeps of equal amplitude: $[t_n, t_{n+\alpha}]$ and $[t_{n+\alpha}, t_{n+1}]$ in order to update the solution substep by substep. Both double step algorithms use a standard backward Euler integration scheme along the first substep and are therefore both midpoint yield consistent.

In the second substep, the DMPT1 algorithm adopts a return map update based on a projection along the midpoint normal-to-yield-surface direction onto the endpoint limit surface. In the second substep, the DMPT2 scheme, instead, adopts an endpoint radial projection combined with a non standard trial state derived from the values of the history variables computed in the first substep and assuming a linear evolution in time over the whole time step. As a result both the DMPT1 and the DMPT2 present midpoint and endpoint yield consistency, which results in evaluating twice the plastic consistency parameter and on an augmented computational effort.

The midpoint algorithm presented for the non-associative J_2 model mainly follows the same lines of the SMPT1 scheme. The only difference lays in the fact that also the evolution equation for the backstress must be integrated in time at each substep and in that this history variable is now updated independently rather than in terms of the deviatoric plastic strain [8]. As previously, the method is based on a single step generalized midpoint integration rule combined with a return mapping algorithm. The return map is achieved enforcing consistency at the end of the time step and projecting the trial solution onto the updated yield surface at the end of each elastoplastic step.

We note that in particular, the generalized integration rule investigated by Ortiz and Popov [2,3] can be specialized to two different methods, namely the proper midpoint integration scheme [3] and the well known backward Euler integration scheme [2,4]. Each of the above integration procedure make use of the return mapping concept as a means to the yield consistency enforcement at the end of the time step. The scheme under consideration will be referred to in the following as the MPTnl method.

3.3 Exponential-based integration algorithms

The stated problem, either with the associative or non-associative flow rule, can be put into a different form by combining Equations (2) and (3), deriving with respect to time and subsequently introducing Equations (5) and (7) respectively. Such calculations lead to the definition of a scalar integration factor X_0 which depends on γ and on the hardening parameters and describes the evolution of the yield surface radius σ_y. With this it is stated that the scalar integration factor plays the role of controlling the time evolution of the inelastic process.

Defining a generalized stress vector $\mathbf{X}$, in terms of the relative stress S and of the scalar integration factor X_0, it is possible to reformulate the initial differential problem in terms of the a new form for the evolution law of the following kind

$$\dot{\mathbf{X}} = \mathsf{A}\mathbf{X} \tag{9}$$

with the matrix A depending on the vector $\mathbf{X}$ and on the actual phase. The solution of Equation (11) can be approximated using exponential maps in each numerical time step.

A detailed description of the new exponential-based algorithms and the full derivation of system (11) can be found in [5-7]. In what follows we refer to the exponential-based algorithms designed for the associative model as ESC and ESC^2, while ESC^{2}nl is the label for the corresponding scheme in the case of non-associative J_2 plasticity [5-7].

4 Numerical examples

4.1 Bi-axial mixed stress-strain loading history

The first numerical example that is introduced presents the relative error curves for stress and strain computation of a mixed pointwise loading history. The loading history [0, T] = [0, 7] assumes to vary the two strain components indicated in Figure 1 and to keep the remaining stress components zero. The material parameters are E = 7000; $\nu = 0.3$; $\sigma_y = 24.3$, $H_{kin} = 0$; $H_{iso} = 225$; $H_{nl} = 0$. The example clearly refers to the associative case with both isotropic and kinematic linear hardening moduli. The error curves represented in Figures 2 report the total stress and strain errors:

$$E^{\sigma} = \sum_{n=0}^{N} \frac{\left\| \boldsymbol{\sigma}_n - \boldsymbol{\sigma}_n^{ex} \right\|}{\sigma_{y,n}} \qquad E^{\varepsilon} = \sum_{n=0}^{N} 2G \frac{\left\| \boldsymbol{\varepsilon}_n - \boldsymbol{\varepsilon}_n^{ex} \right\|}{\sigma_{y,n}} \tag{10}$$

for different choices of time discretization amplitudes, taking as a reference solution the one computed with the backward Euler method (BE method) with a very fine time discretization [2-4]. The computation of stress and strain with different integration algorithms is carried out using the CE-DRIVER code [9]. The error curves are plotted in bi-logarithmic scale and are made up with five progressively smaller choices of the time discretization step.

The plotted curves emphasize that the exponential-based method ESC^2 produces the lowest error levels within the confronted methods. All the compared procedures, except the SMPT2, show second order accuracy, while the backward Euler shows first-order accuracy. The double-step DMPT2 reveals to be the most precise between the midpoint methods. The endpoint inconsistent single step SMPT2 shows loss of accuracy as the discretization parameter decreases and nearly tends to a linear accuracy pattern. The first-order accurate BE method instead results as a first-order accurate method and grants the lowest precision within compared methods.

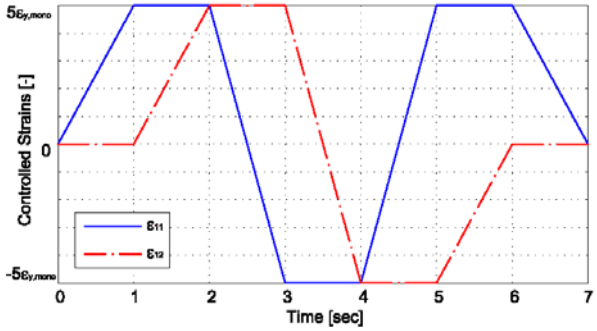

Fig. 1 Mixed stress-strain loading history: time evolution of controlled strains.

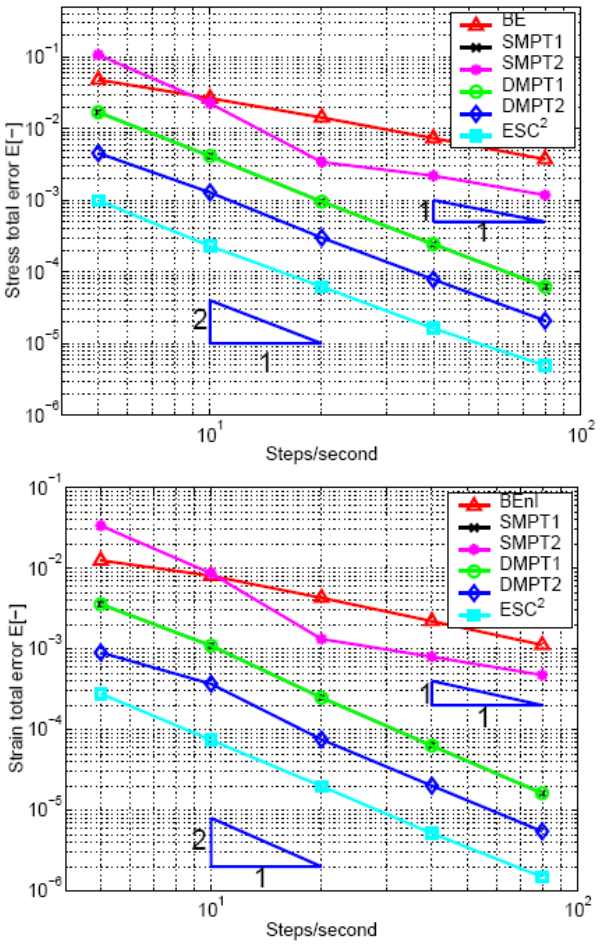

Fig. 2 Pointwise stress-strain test. Stress and strain total error versus number of steps per second.

4.2 Perforated plane strain tension strip

The second numerical simulation regards an initial equilibrium boundary value problem of a rectangular strip with a circular hole in plane strain regime under tension. The system has two axes of symmetry and due to the symmetry of loading only a quarter of the strip is examined, as depicted in Figure 3. The

geometric lengths are $B = 100$, $H = 180$, $R_0 = 50$. The material constants are taken as the previous ones, plus the material has a nonlinear kinematic hardening $H_{nl} = 50$. The loading history consists of imposing a uniform vertical displacement to the upper side $\delta(t)$, up to a maximum size of $0.02\ B$ in 1 time unit within equal increments. The left and bottom sides are fixed with rollers which block transverse displacements respecting the symmetry condition while the right side is free.

The problem is solved using a finite element strategy through the code FEAP [10-11] in conjunction with a Newton-Raphson iterative solver. The mesh consists of 194 SOLID2D finite element in plane strain regime. The comparison of the algorithms is carried out choosing different time integration amplitudes and measuring the error on the computation of displacement using such discretizations referring to an exact solution calculated using the Backward Euler method and a very fine time discretization. The results resumed in Table 1 report the total error horizontal displacement of the hole superior apex, using the ESC^{2}nl and the MPTnl methods with different time discretizations and the non-associative variant of the backward Euler method (BEnl) as reported in reference [2-4]. It is evident that the MPTnl and the ESC2nl still show second-order accuracy, while the backward Euler BEnl method presents first-order accuracy. Namely, in the first two cases the relative error on the displacement goes as Δt^2, while in the third case the error goes as Δt. The comparison between the second-order accurate methods for non-associative plasticity refers practically equal results. For practical computation thus one is lead to involve other considerations than simply accuracy and precision as for instance simplicity in coding the integration algorithm and computational time. In regard to this point it is noted that the midpoint method basically results as the lighter procedure and especially for the greater simplicity of the relative consistent tangent operator. The ESC^{2}nl procedure on the other hand does not involve the solution of a consistency equation which in the case of the MPTnl method results highly nonlinear and therefore represents the bottle neck of the procedure in terms of computational effort.

Tab. 1 Relative error: strip with hole boundary value problem

Δt	BEnl	MPTnl	ESC^{2}nl
.1	5.0×10^{-3}	2.2×10^{-4}	2.1×10^{-4}
.05	2.5×10^{-3}	5.7×10^{-5}	5.1×10^{-5}
.025	1.3×10^{-3}	1.5×10^{-5}	1.2×10^{-5}

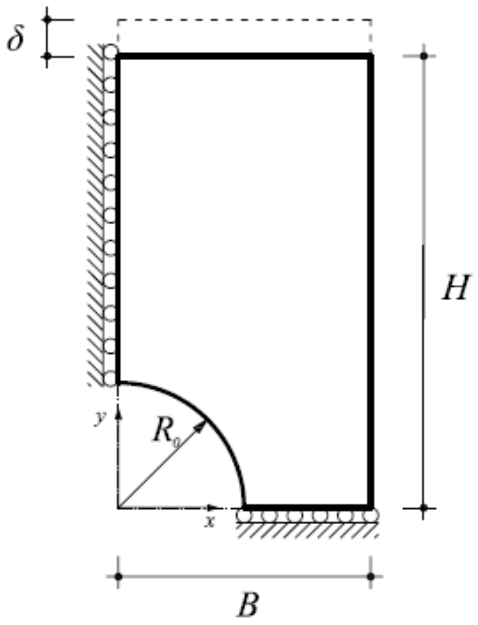

Fig. 3 Perforated strip with upper side imposed displacement.

5 References

[1] P.J. Armstrong, C.O. Frederick. A mathematical representation of the multi-axial baushinger effect. Technical Report C.E.G.B. Report RD/B/N731, Berkeley Nuclear Laboratories, R&D Department, 1966

[2] M. Ortiz, W. Popov, Accuracy and stability of integration algorithms for elastoplastic constitutive relations. International Journal for Numerical Methods in Engineering, 21, 1561-1577, 1985.

[3] J.C. Simo, R.L. Taylor, A return mapping algorithm for plane stress elastoplasticity. International Journal for Numerical Methods in Engineering, 22, 649-670, 1986.

[4] J.C. Simo, Numerical analysis and simulation of plasticity. Handbook of numerical Analysis, P.G. Ciarlet and J.L. Liond Eds., Elsevier, 1998.

[5] E. Artioli, F. Auricchio, L. Beirão da Veiga; Integration Schemes for von Mises Plasticity models based on exponential maps: numerical investigations and theoretical considerations, International Journal for Numerical Methods in Engineering, 64(9), 1133-1165, 2005.

[6] E. Artioli, F. Auricchio, L. Beirão da Veiga; "A novel 'optimal' exponential-based integration algorithm for von-Mises plasticity with linear hardening: Theoretical analysis on yield consistency, accuracy, convergence and numerical investigations", International Journal for Numerical Methods in Engineering, 67(4), 449-498, 2006.

[7] E. Artioli, F. Auricchio, L. Beirão da Veiga; Second-order accurate integration algorithms for von-Mises plasticity with a nonlinear kinematic hardening mechanism, Computer Methods in Applied Mechanics and Engineering, 196, 1827-1846, 2007.

[8] E. Artioli, F. Auricchio, L. Beirão da Veiga; Generalized midpoint integration algorithms for J2 plasticity with linear hardening, International Journal for Numerical Methods in Engineering, in press, 2007.

[9] F. Auricchio. Ce-driver. Technical report, Dipartimento di Meccanica Strutturale – University of Pavia, 2001. Manual prepared for the European School of Advanced Studies of Seismic Risk Reduction.

[10] R.L. Taylor. A finite element analysis program. Version 7.5 user manual. Technical report, University of California at Berkeley, 2003. http://www.ce.berkeley.edu/rlt.

[11] O.C. Zienkiewicz and R.L. Taylor. The finite element method, volume II. McGraw Hill, New York, fifth edition, 2002.